Supporting Information for

Lithographically fabricated gold nanowire waveguides for plasmonic routers and logic gates

Long Gao,[a,b] Li Chen,[a] Hong Wei*[a] and Hongxing Xu[c]

[a]Beijing National Laboratory for Condensed Matter Physics, Institute of Physics, Chinese Academy of Sciences, Beijing 100190, China

[b]School of Physical Sciences, University of Chinese Academy of Sciences, Beijing 100049, China

[c]School of Physics and Technology and Institute for Advanced Studies, Wuhan University, Wuhan 430072, China

*E-mail: weihong@iphy.ac.cn

1. Influence of adhesion layer, Al_2O_3 coating layer, and annealing effect on the SP propagation on gold NWs

Three pieces of samples with gold NWs are fabricated by the lithographic method. The thickness of the gold film for the three samples is 150 nm. For the first sample, a 5 nm thick chromium film is deposited as the adhesion layer before depositing the gold film. For the second sample, only gold is deposited. The gold NWs without adhesion layer on the third sample are coated by a 10 nm thick Al_2O_3 layer. SPs propagating on the NW are launched by focusing a laser beam of 800 nm wavelength at one end of the NW through an objective (×100, NA=0.9) and the scattering light from the distal end of the NW is collected by the same objective and detected by a CCD camera.

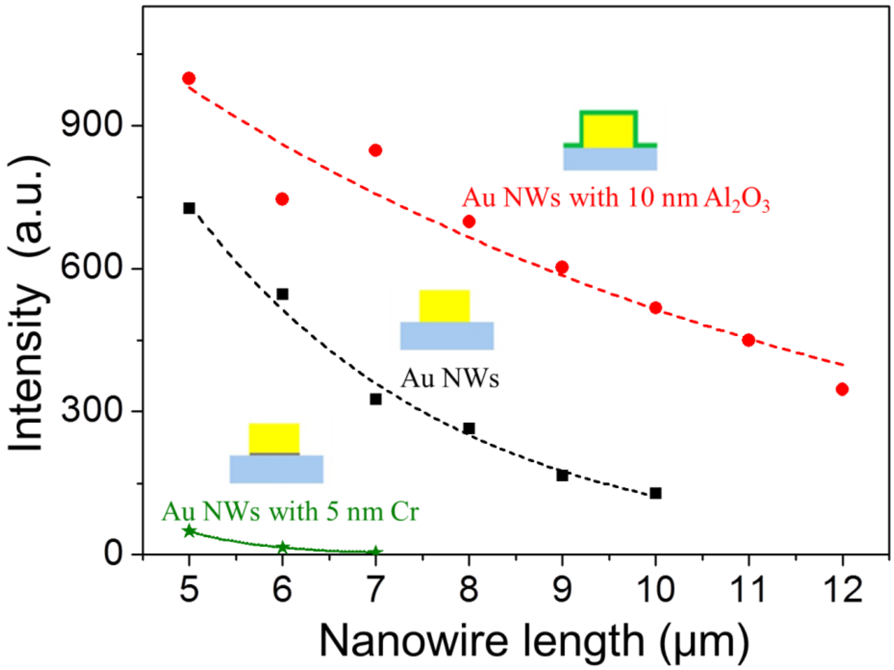

Figure S1. Intensity of SP scattering light from the distal ends of gold NWs excited by laser light of 800 nm wavelength. The gold thickness is 150 nm, and the NW width is about 120 nm.

Figure S1 shows the SP scattering intensity of different samples. When there is a 5 nm adhesion layer of chromium underneath, the SP scattering intensity (green stars) is less than one-tenth of the intensity for the sample without adhesion layer (black squares). For the NWs with a 10 nm thick Al_2O_3 coating layer, the SP scattering intensity (red circles) shows a large increase compared to the sample without Al_2O_3 coating layer.

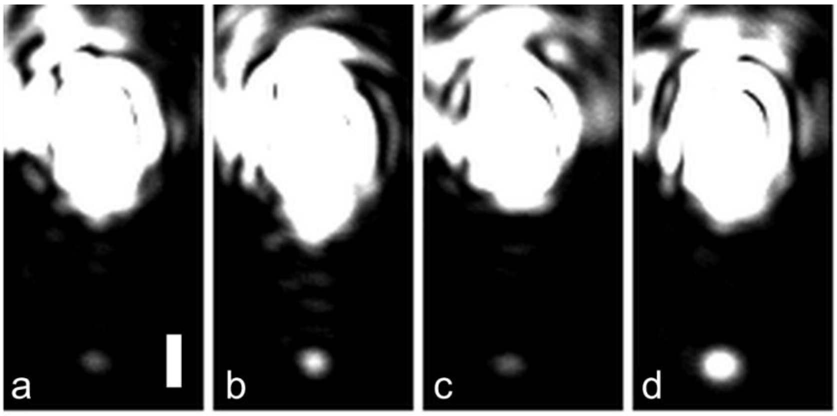

Figure S2. (a, b) Scattering images of a gold NW before (a) and after (b) depositing 10 nm Al_2O_3. (c, d) Scattering images of a gold NW before (c) and after (d) the annealing. The SPs are excited by focusing the laser light of 785 nm wavelength at the end of the NW through an objective (×100, NA=0.9). The polarization of the laser light is parallel to the NW. The scale bar is 1 μm.

The enhancement of the SP scattering intensity for the NWs coated by Al_2O_3 should come from the annealing effect induced structural modifications on the NWs, as the sample is placed in the reaction chamber heated to 200 ^{o}C for atomic layer deposition. To prove this speculation, we fabricate two samples. The thickness of the gold NWs is 150 nm. One sample is coated by Al_2O_3 of 10 nm thickness, while the other sample is placed in the chamber at 200 ^{o}C for 30 min without depositing Al_2O_3. Figure S2 shows the scattering images for gold NWs of 5 μm long before and after depositing Al_2O_3 (Figure S2a, b) and mere annealing (Figure S2c, d). As can be seen, the SP scattering intensity for both samples is increased while the enhancement factor is different. The gold NWs treated with mere annealing without depositing Al_2O_3 show larger enhancement of the SP scattering intensity. Measurements for five NWs on each sample show that the enhancement factor of the SP scattering intensity for the sample with and without Al_2O_3 is 2.2 and 4.2, respectively.

From the mode analysis, we obtain the effective refractive indices of the SP modes $n_{\mathrm{eff}} = n' + in''$ for different Al_2O_3 thicknesses. The SP propagation length L_{SP} is determined by the imaginary part of the effective refractive index: $L_{\mathrm{SP}} = 1/(2k_0 n'')$, where k_0 is the wave vector in vacuum corresponding to 785 nm wavelength. Figure S3 shows the propagation length of different SP modes as a function of Al_2O_3 layer thickness. As can be seen, the propagation length is decreased with the increase of Al_2O_3 thickness, because the SP modes are more tightly confined on the gold for thicker Al_2O_3. These results indicate that the annealing leads to the decrease of the SP loss and the Al_2O_3 layer actually increases the SP loss. Because of the absence of adhesion layer, a coating layer is still necessary for immobilizing and protecting the NWs. For this reason, we keep the 10 nm Al_2O_3 coating layer in our samples.

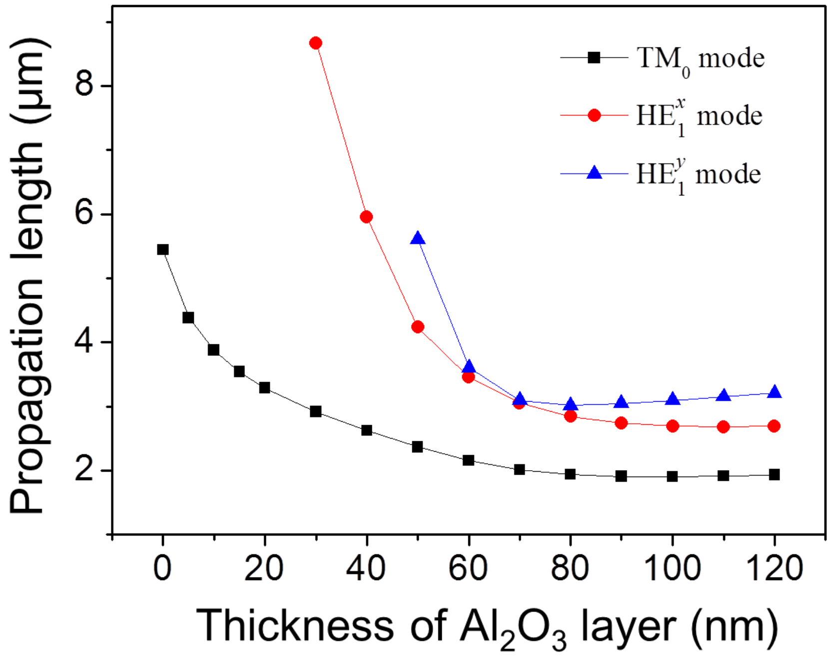

Figure S3. Calculated propagation length of SP modes as a function of Al_2O_3 layer thickness. The gold NWs are placed on a substrate with refractive index of 1.518. The width and height of the NWs are both 150 nm. The wavelength is 785 nm.

2. Fitting method for the SP scattering intensity as a function of NW length

For gold NWs placed in a homogeneous surrounding medium, a strong oscillation of the output scattering intensity versus the NW length is observed (Figure 2b). For excitation light polarized parallel to the NW, TM_0 mode and HE_1^y mode can be excited simultaneously. The superposition of these two modes leads to a zigzag distribution of electric field on the top and bottom of the NW.[1] Since the radiation pattern from the output end is highly dependent on the near field distribution, the intensity collected by the objective varies with the length of the NW. The period of the zigzag pattern on the NW Λ is inversely proportional to the difference between the real part of the effective refractive index of TM_0 mode and HE_1^y mode: $\Lambda = \lambda/(\mathrm{Re}(n_1) - \mathrm{Re}(n_2))$, where λ is the wavelength of the excitation light, and n_1 and n_2 are the effective refractive index of TM_0 mode and HE_1^y mode, respectively. The near field intensity on the top side of the NW end can be considered as

$$I_{\mathrm{top}} = |E_1 e^{ik_1 l} e^{\mathrm{i}\varphi_1} + E_2 e^{ik_2 l} e^{i\varphi_2}|^2, \qquad (1)$$

where E_1 and E_2 represent the electric field amplitude of TM_0 mode and HE_1^y mode, respectively; $k_1 = n_1 k_0$ and $k_2 = n_2 k_0$ are the corresponding wave vectors of the two modes; l is the length of the NW; φ_1 and φ_2 are the initial phases of the two modes. The initial phase difference $\varphi_1 - \varphi_2$ is assumed to be $\pi/2$ and φ_1 is set to be 0. From the mode analysis, we obtain $k_1 = \frac{2\pi}{\lambda}(1.9328 + 0.02478\mathrm{i})$, and $k_2 = \frac{2\pi}{\lambda}(1.614 + 0.01142\mathrm{i})$, where λ is 785 nm. The blue dashed curve in Figure 2b is the fitting result using equation (1).

3. SP scattering intensity in the Y-shaped NW network as a function of incident polarization angle

For the Y-shaped NW networks shown in Figure 3, we measured the dependence of the output intensity of the two branches on the incident polarization angle (Figure S4a, c and e). The optimal polarization angle θ for the maximal intensity ratio of the two output ends is found to be around $\pm 60°$ for the Y-shaped NW networks with the main wire length of 3.4 μm and 4.6 μm (Figure S4b and f). The switching ratio for the structure with the main wire length of 4 μm is relatively low, and the polarization angles for high switching ratio correspond to very low SP output intensity at the ends of the two branches. Therefore, this structure is not suitable for SP routing. The SP routing behavior is determined by the electric field intensity on the two sides of the branch junction. For the TM_0 mode, the field amplitude and phase are the same on the two sides of the junction, while for the HE_1^x mode, the field has a phase difference of π on the two sides of the junction. For the polarization angle $\theta = 0°$, the TM_0 mode is excited, while for $\theta = 90°$, the HE_1^x mode is excited. Figure S5a shows the electric field amplitude of the two modes as a function of the polarization angle of the excitation light with the maximum field amplitude of the two modes the same. The field amplitude of the two modes is the same for $\theta = \pm 45°$, which leads to the largest intensity ratio of the two branches at $\theta = \pm 45°$ due to the superposition of the two modes (Figure S5b). However, in the experiment, the electric field amplitude of the two modes under excitation with $\theta = \pm 45°$ is not the same, which leads to a shift in the polarization angle for the largest switching ratio. By setting the maximum amplitude ratio of the TM_0 and HE_1^x modes to be 2:1, the field amplitude of the two modes is the same for $\theta = \pm 63.4°$ (Figure S5c). Therefore, the superposition of the two modes results in the maximum switching ratio of the two branches at $\theta = \pm 63.4°$ (Figure S5d). As can be seen, the line shape of the field intensity on the two sides of the junction in Figure S5d is similar to the experimental result in Figure S4a for the Y-shaped NW network with the main wire length of 3.4 μm.

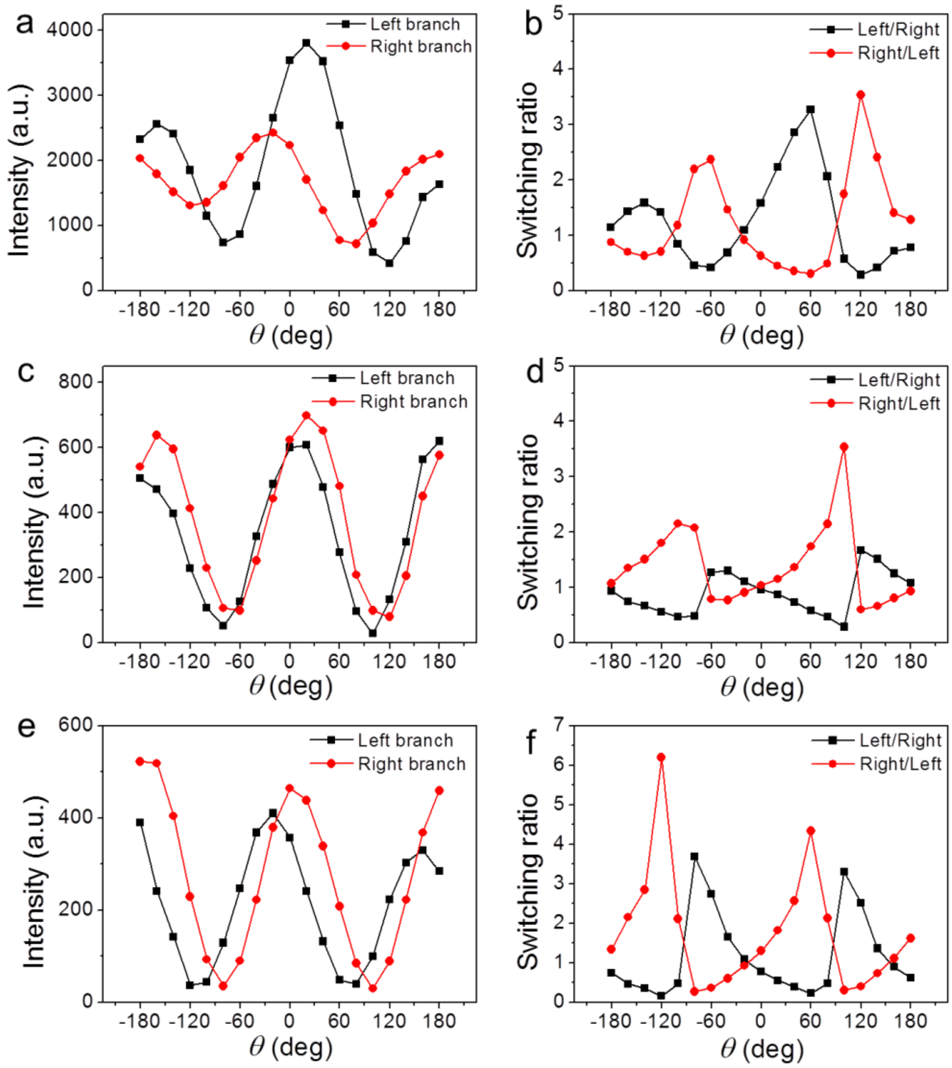

Figure S4. Output intensity (a, c, e) and switching ratio (b, d, f) of two branches in the Y-shaped NW networks with different main wire lengths as a function of the polarization angle of the excitation light. The length of the main wire is (a, b) 3.4 μm, (c, d) 4 μm, and (e, f) 4.6 μm. The wavelength of the excitation light is 785 nm.

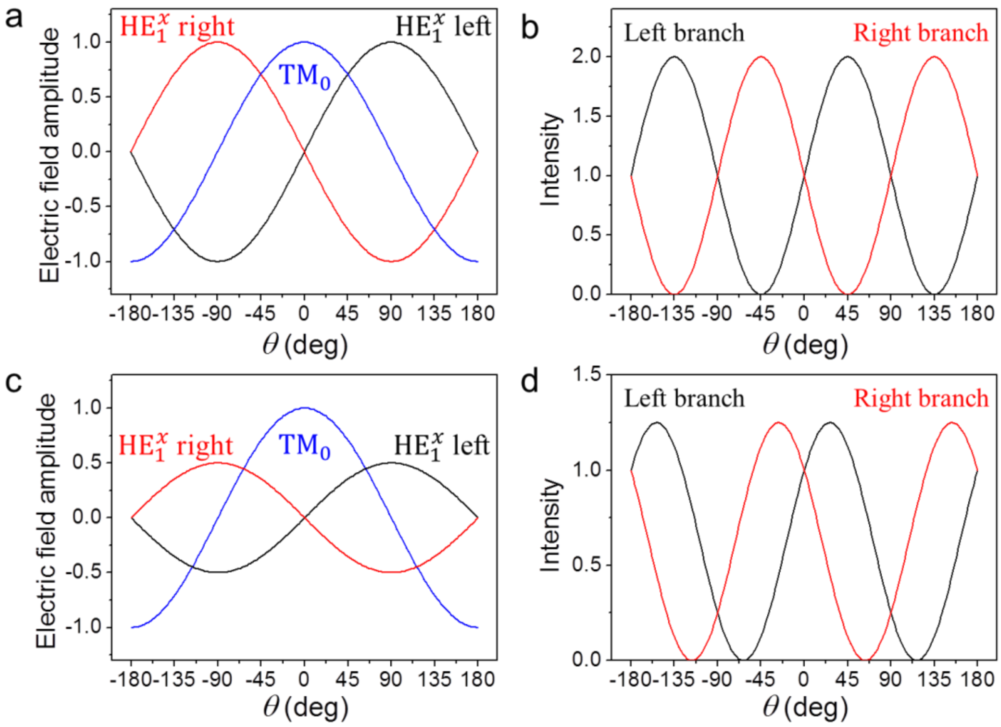

Figure S5. (a) Electric field amplitude of TM_0 and HE_1^x modes on the two sides of the NW junction. The field amplitude of TM_0 and HE_1^x modes are simulated by $\cos\theta$ (blue line) and $\pm\sin\theta$ (black and red lines), respectively. The amplitude ratio of TM_0 and HE_1^x modes is set to be 1:1. (b) Electric field intensity on the two sides of the NW junction resulting from the superposition of TM_0 and HE_1^x modes corresponding to (a). (c) Electric field amplitude of TM_0 and HE_1^x modes with a ratio of 2:1. (d) Electric field intensity on the two sides of the NW junction corresponding to (c).

4. Demonstration of plasmonic NAND and NOR gates by cascading AND and OR gates with NOT gate

Except the realization methods we described in the article, NAND and NOR gates can also be obtained by cascading AND and OR gates with NOT gate. The cascaded NAND and NOR gates can be realized in the four-terminal NW network as we used in the article but with different input power ratio. The I1 and I2 ends are the two input ends for AND or OR gate (Figure S6a). The operation results of AND or OR gate becomes the input of NOT gate. The end C is the input end for the control signal which inverts the input signal of NOT gate. When the control signal is turned off, the device can execute the AND or OR logic operations. When the control signal is turned on, the device can execute the NAND or NOR logic operations.

Figure S6b demonstrates the output intensity versus the phase difference of the inputs for the cascaded NAND gate. The intensity ratio of O(I1), O(I2) and O(C) is set to be 1:1:9 (the intensity of O(I1) and O(I2) is about 100 and the intensity of O(C) is about 900), which means the amplitude ratio of electric field of the output is 1:1:3. When the I1 and C inputs are turned on and the phase of the I1 input is tuned, the interference leads to the oscillation of the output intensity O(I1, C). The destructive interference leads to the minimum of O(I1, C) with the intensity 4 times as high as O(I1). Then I1 input is blocked and I2 input is turned on. Tuning the phase of I2 can lead to the minimum of O(I2, C) for destructive interference which is close to O(I1, C). Then the C input is blocked and I1 is turned on again, which results in the intensity of O(I1, I2) similar to O(I2, C). By tuning the phase of I2, we find that this intensity of O(I1, I2) is the maximum value. Finally all three inputs are turned on, and O(I1, I2, C) is at the minimum value as confirmed by tuning the phase of I2 input. Now the phase of I1 and I2 inputs are fixed, which correspond to constructive interference of I1 with I2 and destructive interference of both I1 and I2 with C. By setting the threshold intensity I_t to 300, the NW network works as a NAND gate cascaded by AND and NOT gates, as shown by the scattering images in Figure S6c.

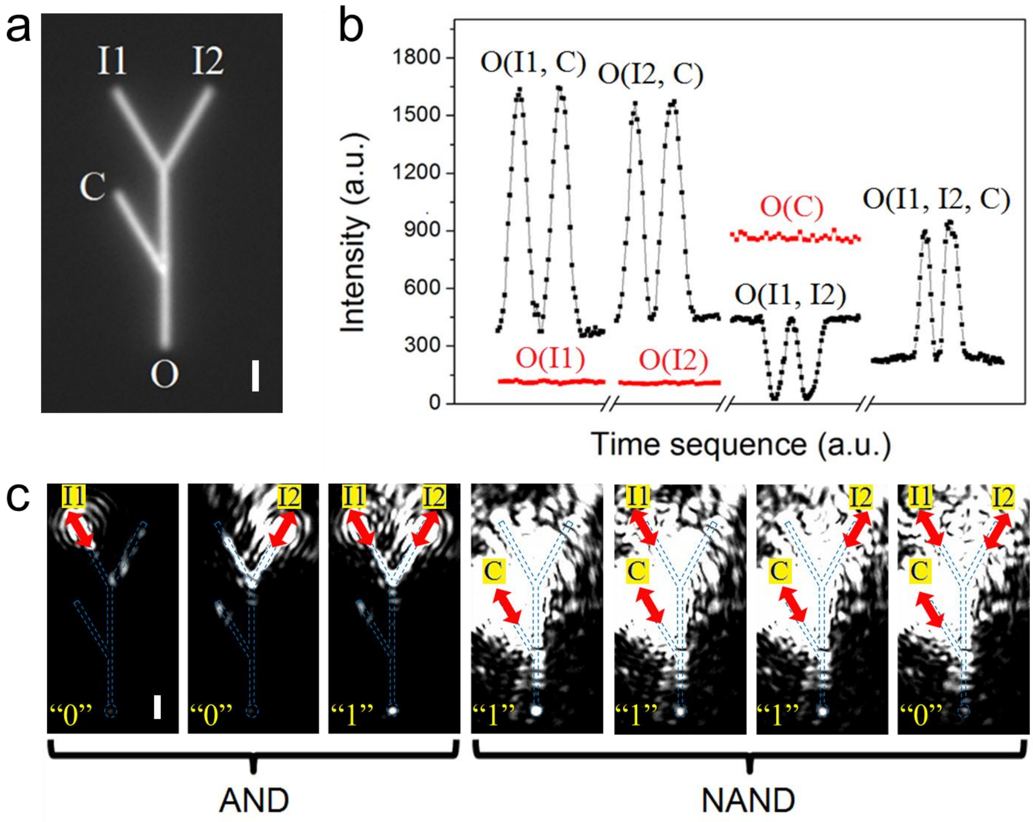

Figure S6. Cascaded NAND logic gate. (a) Optical image of the gold NW network. (b) Output intensity for single inputs (red) and multiple inputs (black) with the phase difference changing over time. (c) Scattering images showing AND and NAND operations. The red arrows indicate the polarization of the input light. The output states are marked as "0" or "1". The scale bars in (a) and (c) are 1 μm.

Figure S7a shows the output intensity versus the phase difference of the inputs for a cascaded NOR gate. Here the intensity ratio of O(I1), O(I2) and O(C) is set to be 1:1:2 (the intensity of O(I1) and O(I2) is about 210 and the intensity of O(C) is about 430). The measurement for the output intensity versus the phase difference of the inputs is similar to that for NAND gate in Figure S6. The I_t is defined as 190, which is below O(I1) and O(I2) and above O(I1, I2, C). Figure S7b shows the scattering images when the structure executes the OR and NOR logic operations, demonstrating that the NOR gate is cascaded by OR and NOT gates.

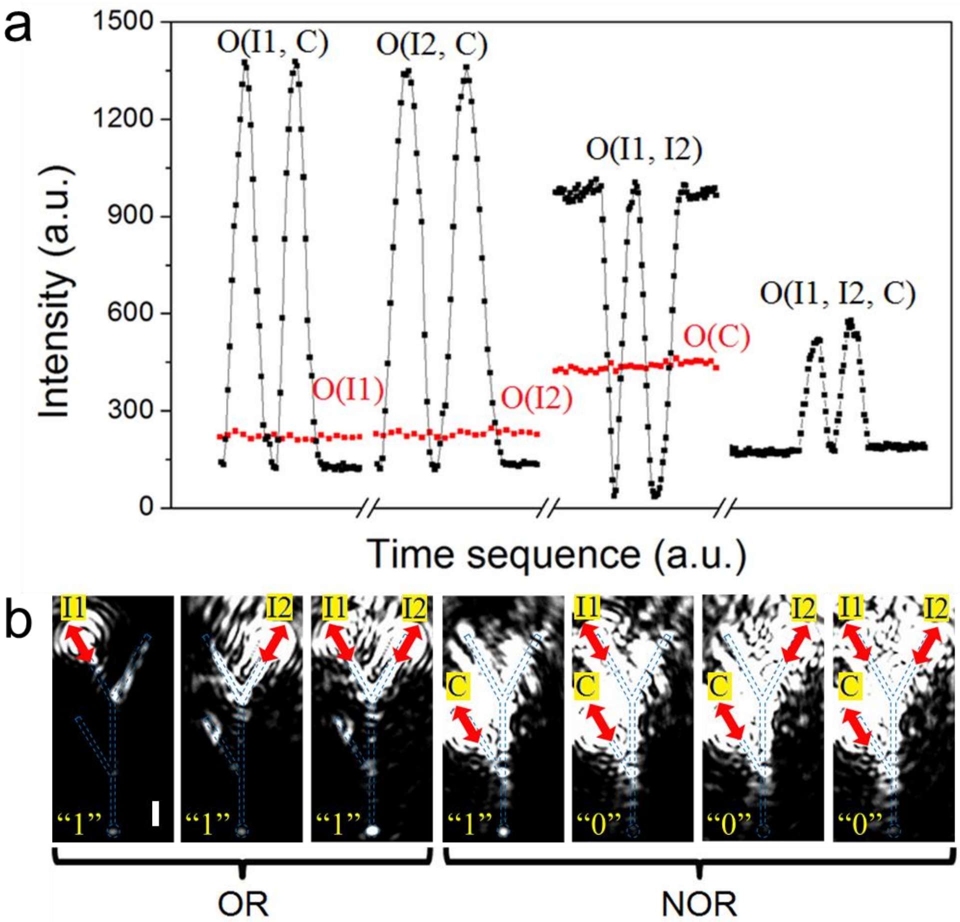

Figure S7. Cascaded NOR logic gate. (a) Output intensity for single inputs (red) and multiple inputs (black) with the phase difference changing over time. (b) Scattering images showing OR and NOR operations. The red arrows indicate the polarization of the input light. The output states are marked as "0" or "1". The scale bar is 1 μm.

Reference

(1) H. Wei, D. Pan and H. X. Xu, *Nanoscale*, 2015, **7**, 19053-19059.